

# Continuous and Scalable Fabrication of Bioinspired Dry Adhesives via a Roll-to-Roll Process with Modulated Ultraviolet-Curable Resin

Hoon Yi,<sup>†,∇</sup> Insol Hwang,<sup>†,∇</sup> Jeong Hyeon Lee,<sup>‡</sup> Dael Lee,<sup>†</sup> Haneol Lim,<sup>§</sup> Dongha Tahk,<sup>§</sup> Minhong Sung,<sup>†</sup> Won-Gyu Bae,<sup>||</sup> Se-Jin Choi,<sup>⊥</sup> Moon Kyu Kwak,<sup>\*,‡</sup> and Hoon Eui Jeong<sup>\*,†</sup>

<sup>†</sup>Department of Mechanical Engineering, Ulsan National Institute of Science and Technology, Ulsan 689-798, Republic of Korea

<sup>‡</sup>Department of Mechanical Engineering, Kyungpook National University, Daegu 702-701, Republic of Korea

<sup>§</sup>Minuta Technology Company, Ltd, Gyeonggi 447-210, Republic of Korea

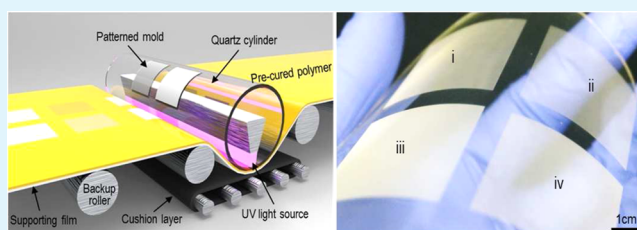
<sup>||</sup>Interdisciplinary Program of Bioengineering, Seoul National University, Seoul 151-742, Republic of Korea

<sup>⊥</sup>MCNet Company, Ltd, Gyeonggi 435-833, Republic of Korea

## Supporting Information

**ABSTRACT:** A simple yet scalable strategy for fabricating dry adhesives with mushroom-shaped micropillars is achieved by a combination of the roll-to-roll process and modulated UV-curable elastic poly(urethane acrylate) (e-PUA) resin. The e-PUA combines the major benefits of commercial PUA and poly(dimethylsiloxane) (PDMS). It not only can be cured within a few seconds like commercial PUA but also possesses good mechanical properties comparable to those of PDMS. A roll-type fabrication system equipped with a rollable mold and a UV exposure unit is also developed for the continuous process. By integrating the roll-to-roll process with the e-PUA, dry adhesives with spatulate tips in the form of a thin flexible film can be generated in a highly continuous and scalable manner. The fabricated dry adhesives with mushroom-shaped microstructures exhibit a strong pull-off strength of up to  $\sim 38.7 \text{ N cm}^{-2}$  on the glass surface as well as high durability without any noticeable degradation. Furthermore, an automated substrate transportation system equipped with the dry adhesives can transport a 300 mm Si wafer over 10 000 repeating cycles with high accuracy.

**KEYWORDS:** micropillar, dry adhesive, gecko, biomimetics, roll-to-roll process



## INTRODUCTION

Micro- or nanostructures with thin film-shaped tips on the feet of climbing creatures contribute to their remarkable adhesion capabilities. In the past decade, significant advancements have been made toward our understanding of the mechanism underlying such adhesion.<sup>1–6</sup> Micro- or nanostructures with a protruding thin-film tip can exhibit superior adhesion properties in comparison to chemical-based ones because the adhesion force mainly originates from intermolecular interactions between the tips and the contact surface, where attractive van der Waals forces exist.<sup>1–11</sup> Furthermore, they allow for reversible and repeatable adhesion to surfaces of varying roughness and orientation.<sup>7,12–21</sup> Motivated by such fascinating properties, many research groups have developed useful fabrication methods based on various top-down and bottom-up approaches. For example, it is now possible to fabricate multiscale hierarchical structures with controlled geometry to accurately imitate the smart adhesion properties of a gecko.<sup>6–10,17–25</sup> Our group has also demonstrated that gecko-inspired angled multilevel hairy structures with directional and reversible adhesion properties can be generated by the two-step ultraviolet (UV) molding technique.<sup>8,18–20</sup> A potential shortcoming of such angled and/or hierarchical nanostructures is that normal adhesion is weak, typically less

than  $\sim 3 \text{ N cm}^{-2}$ .<sup>7,18–20,26</sup> Moreover, these structures are easily collapsed after repeated use.<sup>20,27,28</sup> More importantly, they are not scalable with current manufacturing techniques.

To address this issue, beetle-inspired microscale structures with mushroom-shaped tips have been proposed as an efficient form for a biomimetic dry adhesive.<sup>1,6,29–31</sup> Recent theoretical and experimental studies demonstrated that the pull-off force of mushroom-shaped microstructures is about 2–30 times higher than that of pillars with simple flat or hemispherical heads because of the enhanced contact area, pollution tolerance, homogeneous stress distribution, and prevention of crack propagation.<sup>1,6,7,12,32,33</sup> Furthermore, the simple microscale structure is relatively easy to produce in a scalable manner and also mechanically more durable as compared with the slanted hierarchical hairy nanostructures. To fabricate mushroomlike microstructures, poly(dimethylsiloxane) (PDMS) or polyurethane (PU) is generally utilized because their favorable mechanical properties (low elastic modulus and high elongation at break) allow for simple prototyping and enhanced normal and shear adhesion strength.<sup>7,12,17,34–36</sup> Nonetheless, they

Received: June 18, 2014

Accepted: August 4, 2014

Published: August 13, 2014

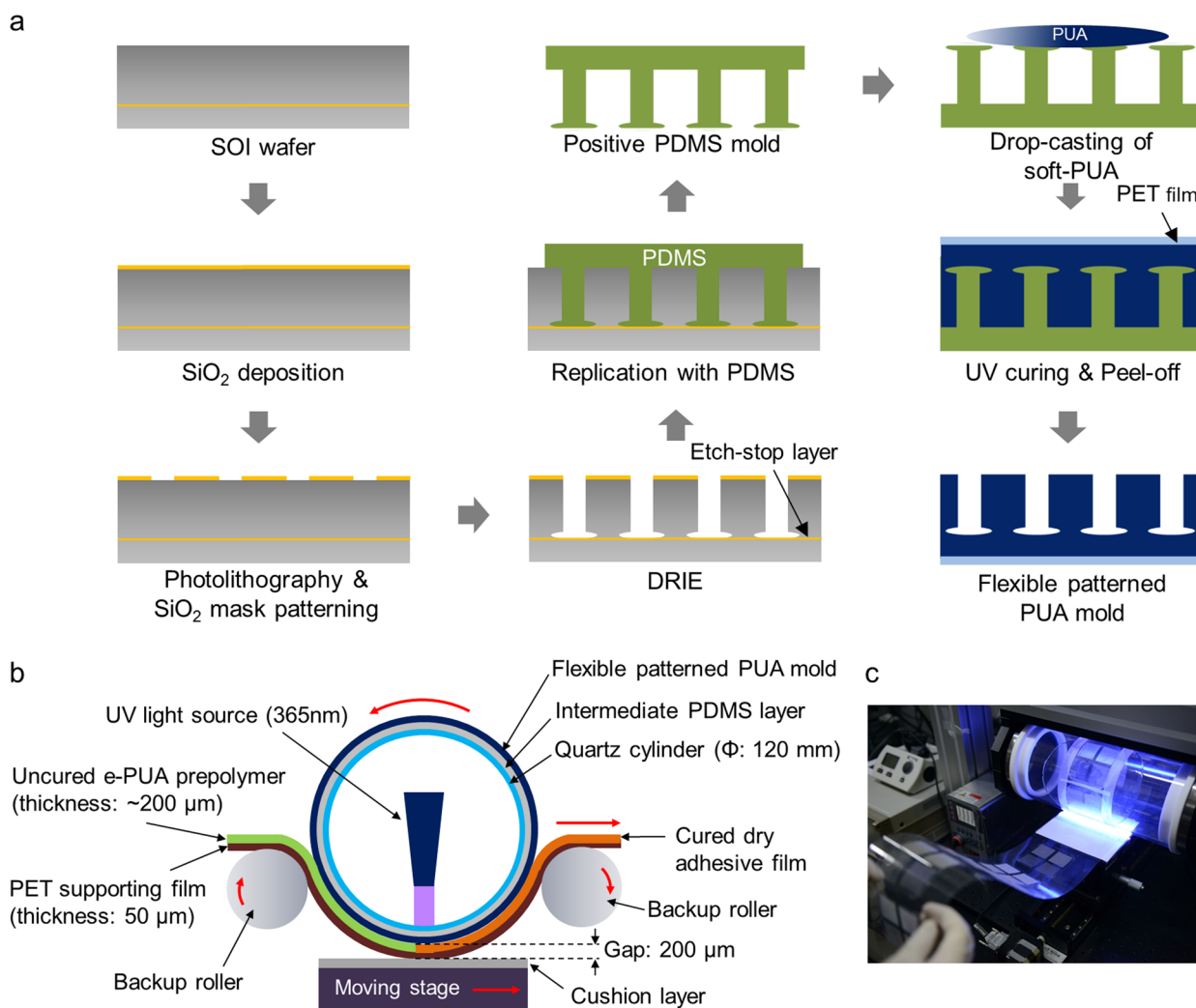


**Figure 1.** (a) Schematic illustration for the fabrication of flexible patterned PUA mold. (b) Schematic description of the roll-type continuous fabrication system; a flexible patterned mold made of soft PUA is adhered to the hollow quartz cylinder inside which a collimated UV light source is mounted. As the UV light is exposed through the slit on the passing substrate coated with the e-PUA, complementary structures of the patterned soft PUA mold are continuously generated in the prepolymer layer. (c) A photograph of the roll-to-roll process demonstrating the continuous fabrication of a dry adhesive film in which mushroomlike micropillars with four different geometries are embedded. The production width was  $\sim 10$  cm, and the speed was about  $\sim 4$  cm  $s^{-1}$ , therefore production capacity reached  $\sim 40$  cm<sup>2</sup>  $s^{-1}$ .

typically require a long curing time (e.g., 1–2 h for PDMS and 1–24 h for PU) at an elevated temperature (i.e., 70–80 °C for PDMS), which significantly hinders practical use and commercialization of the dry adhesive materials.<sup>7,12,17,34,35</sup> Also, commercially available UV resins typically have high tensile modulus and low elongation at break, which could result in demolding failure of micropillars with protruding spatulate tips and low pull-off strength of the replicated structures. In fact, although our group proposed a UV molding technique in which a bioinspired nanostructure with controlled leaning angle and hierarchy could be generated in a few tens of seconds by utilizing commercial poly(urethane acrylate) (PUA),<sup>8,18–20</sup> we could not fabricate the mushroomlike microstructures using the material because of demolding failure or the low pull-off strength of the replicated structure, mainly induced by the nonoptimized mechanical properties of the UV resin (i.e., high tensile modulus and low elongation at break).

In this study, we report a continuous fabrication of bioinspired dry adhesives with mushroomlike micropillars by utilizing a roll-to-roll process and modulated elastic PUA (e-

PUA). The e-PUA combined the major benefits of commercial PUA and PDMS. It not only can be cured within a few seconds like commercial PUA but also possesses good mechanical properties (low elastic modulus and high elongation at break) comparable to those of PDMS. A roll-type fabrication system equipped with a rollable mold and a UV exposure unit was developed for the continuous process. By integrating the roll-to-roll process with the e-PUA, dry adhesives with spatulate tips in the form of a thin flexible film can be generated in a highly continuous and scalable manner. The fabricated mushroomlike microstructures with controlled geometries exhibit good structural integrity, pull-off strength, and structural durability. Furthermore, an automated substrate transportation system equipped with the dry adhesives can transport a large area substrate over 10 000 repeating cycles with high accuracy.

## EXPERIMENTAL SECTION

**Preparation of e-PUA Mixture.** The UV-curable e-PUA mixture consists of a functionalized prepolymer with acrylate groups for cross-linking, modulators, and a photoinitiator. The prepolymer was aliphatic urethane diacrylate oligomer (SC4240, Miwon Specialty

Chemical). The modulators of bisphenol A (ethoxylated) 10 dimetacrylate (BPA(EO)10DMA, M2101, Miwon Specialty Chemical) and the tri(propylene glycol) diacrylate (M220, Miwon Specialty Chemical) were mixed with the prepolymer at 15 and 6 wt %, respectively. 2-hydroxy-2-methyl-1-phenylpropan-1-one (Darocur 1173, Ciba Specialty Chemical) was added to the mixture as a photoinitiator at 4 wt %.

**Fabrication of Silicon on Insulator Master.** A silicon-on-insulator (SOI) wafer was purchased from Mico SNP Ltd. (Korea). The wafer (p-type, 100) possessed a 1  $\mu\text{m}$  thick oxide layer on a 500  $\mu\text{m}$  thick silicon layer. A 20  $\mu\text{m}$  thick polysilicon layer was then formed over the oxide layer. An 800 nm thick  $\text{SiO}_2$  layer was deposited on the SOI wafer by a plasma-enhanced chemical vapor deposition process with tetraethoxysilane (TEOS). Then, microhole patterns with different diameters and pitches were made by conventional photolithography with AZ1512 photoresist. Subsequently, pattern transfer to the  $\text{SiO}_2$  layer was carried out using the photoresist (PR) etch mask, which was followed by removal of the PR. Then, the polysilicon layer was anisotropically etched via  $\text{SF}_6$  and Ar gas plasma until the exposure of the  $\text{SiO}_2$  etch-stop layer in an inductively coupled plasma (ICP) chamber with 13.56 MHz radio frequency power generators. The same etching was performed further utilizing an extremely high etch selectivity between polysilicon and  $\text{SiO}_2$  etch-stop layer to overetch the polysilicon layer to the lateral direction (Figure 1a). For surface hydrophobization, the patterned wafers were treated with a trichloro-(1H,1H,2H,2H-perfluorooctyl)silane.

**Fabrication of a Patterned Flexible PUA Mold.** After the SOI master was prepared, PDMS micropillars with a spatulate head were obtained by casting the PDMS precursor (Sylgard 184, Dow Corning) over the SOI master with 10% curing agent. To make a flexible negative PUA mold for the roll-to-roll system, drops of soft PUA (MINS 301 RM, Minuta Tech) prepolymer were drop-dispensed onto the replicated PDMS micropillars, and a flexible polyethylene terephthalate (PET) film (thickness  $\approx 50 \mu\text{m}$ ) was slightly pressed against the liquid drop, followed by subsequent UV exposure ( $\lambda = 250\text{--}400 \text{ nm}$ , dose =  $300 \text{ mJ cm}^{-2}$ ). After UV curing, a flexible PUA mold with negative patterns was obtained by peeling it off from the PDMS mold (see Figure 1a). The prepared flexible PUA mold was additionally exposed to UV for several hours to remove trapped polymer radicals and the remaining unsaturated acrylate in the replicated mold so that it could be used for the self-replication of mushroomlike micropillars with UV-curable resins.

**Set-up of the Roll-to-Roll System and Continuous Fabrication of e-PUA Micropillars.** Overall, the roll-to-roll system consists of a flexible patterned mold made of soft PUA, arollable UV exposure unit, and a motorized substrate feeding system. First, the flexible patterned mold was prepared by a simple molding process with the soft PUA as described above. This flexible PUA mold was then conformably adhered to the outer surface of a hollow quartz cylinder using an intermediate thin PDMS layer. The quartz cylinder was rotated by friction or step motor depending on production speed. When the process speed was above 1 cm/s, the motor driving mode was utilized, whereas the friction mode was utilized for lower process speeds. The collimated UV source core was prepared by placing the 5 mm wide slit over the UV lamp (SUV-L, UVSMT). The UV core was suspended inside a 90 mm diameter hollow quartz cylinder with the slit facing downward, supported by ball bearings at both ends of the cylinder so as to allow cylinder rotation with the static UV core inside. A thin layer of PDMS sheet was wrapped around the outer cylinder surface, and then the flexible PUA mold was conformably attached onto the PDMS layer. Therollable UV exposure unit was arranged over a three degrees of freedom stage equipped with a step motor. A substrate coated with e-PUA prepolymer was then located on the motorized linear stage and brought into contact with the patterned PUA mold by controlling the stage axes in such a way that the contact line between the substrate surface and the rolled mold was aligned to the UV exposing slit inside. As the UV light (365 nm wavelength and  $1000 \text{ mW/cm}^2$  intensity) was exposed through the slit on the passing substrate, complementary structures of the flexible PUA mold were generated continuously in the pre-polymer layer.

**Fabrication of Soft PUA and PDMS Micropillars with Spatulate Tips.** Soft PUA micropillars and PDMS micropillars were prepared by a simple replica molding process (i.e., discontinuous process). To make micropillars with soft PUA, drops of soft PUA were dispensed onto the flexible negative PUA mold, and a flexible PET film (thickness  $\approx 50 \mu\text{m}$ ) was slightly pressed against the liquid drop to be used as a supporting layer. After UV exposure, the cured soft PUA replica was carefully demolded from the negative mold to avoid possible fracture of the spatulate tips. For PDMS micropillars, a 10:1 mixture of the PDMS prepolymer (Sylgard 184A) and the curing agent (Sylgard 184B) was poured onto the master or the flexible negative PUA mold. Subsequently, the master was placed in a convection oven and cured at  $70 \text{ }^\circ\text{C}$  for 2 h. Finally, the cured PDMS replica was carefully detached from the master.

**Adhesion Measurements.** The pull-off forces of e-PUA micropillars were evaluated by custom-built equipment at a relative humidity of 40% and ambient temperature of  $25 \text{ }^\circ\text{C}$ .<sup>37</sup> A circular adhesive patch (diameter = 7 mm) was attached to a flat glass surface under a controlled preload ranging from 2 to 70 N and was lifted by the motorized stage at the speed of  $1 \text{ mm s}^{-1}$  until separation occurred. For comparison, the pull-off forces of soft PUA and PDMS micropillars (of identical diameter) were also measured in a similar way. For statistical significance, the adhesion measurement was carried out 20 times for each sample under identical conditions.

**Surface Tension Characterization.** To evaluate the surface tension of the soft PUA and the e-PUA, the static contact angles on each planar sample were measured with probing liquids of deionized (DI) water and diiodomethane. The surface tension values of the soft PUA and the e-PUA were then calculated by the harmonic mean method (Table 2).

**Table 1. Comparison of Tensile Modulus and Elongation at Break for Four Materials**

| material | tensile modulus (MPa) | elongation at break (%) |
|----------|-----------------------|-------------------------|
| hard PUA | 320.0                 | 9.0                     |
| soft PUA | 19.8                  | 45.0                    |
| e-PUA    | 10.0                  | 132.2                   |
| PDMS     | 1.6                   | 146.0                   |

## RESULTS AND DISCUSSION

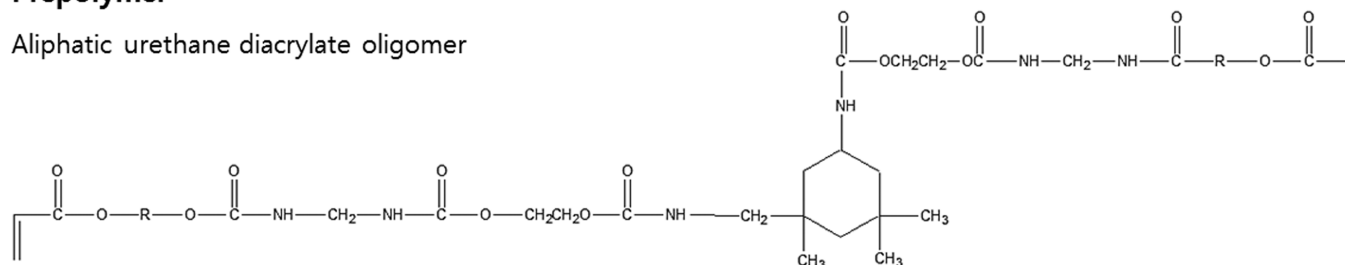
Figure 1b depicts the main components in the roll-type continuous fabrication system: a flexible patterned PUA mold, arollable UV exposure unit, and a motorized substrate feeding system. The flexible patterned mold was made of soft PUA (MINS-301 RM, Minuta Tech) by a simple molding process on a polyethylene terephthalate (PET) sheet (see Experimental Section for the detailed procedure). This flexible soft PUA mold was then conformably adhered to the outer surface of a hollow quartz cylinder using an intermediate thin PDMS layer. Inside this quartz cylinder, a 365 nm wavelength UV light source was mounted and collimated to a 5 mm wide aperture. An uncured PUA prepolymer was coated on the PET substrate by a doctor blade and was then fed to the UV exposure roll, where the contact line between the substrate surface and the roll was aligned to the UV-exposing aperture slit. The production speed is determined by the UV exposure dose that is required to cure the PUA prepolymer. In our experiment, the intensity of the UV source was  $1000 \text{ mW/cm}^2$ , and the width of the exposing slit was 5 mm. Because the required UV dose for the e-PUA is  $\sim 100 \text{ mW/cm}^2$ , the maximum possible rolling speed is  $\sim 5 \text{ cm/s}$ . In this study, the rolling proceeded at speeds of up to 4 cm/s to ensure complete UV curing of the e-PUA with slight over exposure. This speed can be enhanced by using a more powerful UV light source.

**Table 2. Contact Angles of DI Water and Diiodomethane on Various Substrates and the Calculated Surface Tension Values Calculated by the Harmonic Mean Method**

| material | CA (DI water) | CA (diiodomethane) | $r^d$ (mJ m <sup>-2</sup> ) | $r^p$ (mJ m <sup>-2</sup> ) | $r$ (mJ m <sup>-2</sup> ) |
|----------|---------------|--------------------|-----------------------------|-----------------------------|---------------------------|
| soft PUA | 87.9° ± 1°    | 73.0° ± 1°         | 17.3                        | 6.6                         | 23.9                      |
| e-PUA    | 74.3° ± 1°    | 26.3° ± 1°         | 41.2                        | 5.2                         | 46.4                      |
| PDMS     |               |                    |                             |                             | 20.2–21.2                 |

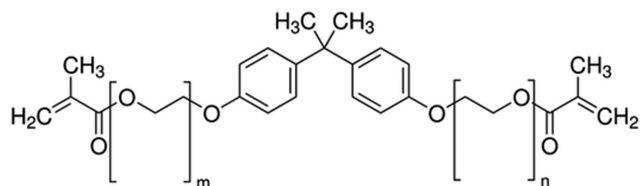
## Prepolymer

Aliphatic urethane diacrylate oligomer

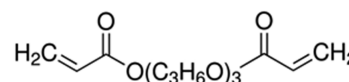


## Modulator

Bisphenol A (ethoxylated) 10 dimethacrylate (BPA(EO)10DMA)



Tri(propylene glycol) diacrylate



## Photoinitiator

2-hydroxy-2-methyl-1-phenylpropan-1-one

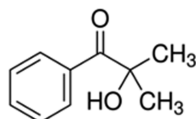


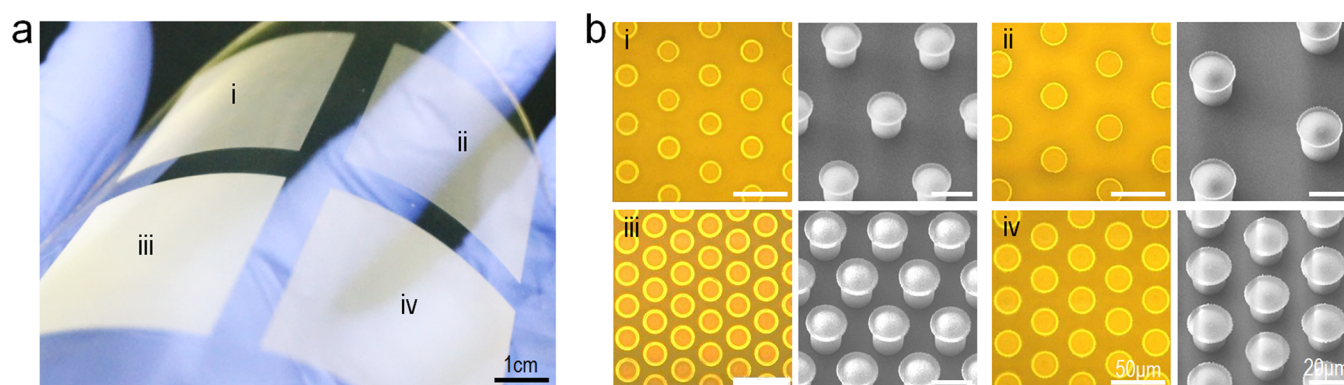
**Figure 2.** Components and chemical formulas of e-PUA, which consists of a prepolymer, modulators, and a photoinitiator.

Here, the rollable mold and the feeding substrate are separated to allow independent motion. When the process speed is above 1 cm/s, the substrate tends to slip on the mold because the uncured prepolymer works as a lubricant.<sup>38</sup> So each motor was controlled consistently for the synchronization of the cylindrical mold and substrate. On the other hand, when the process speed is lower than 1 cm/s, frictional synchronization can be employed in which only one of two driving forces, which rotate the cylinder and the feeding roller, is enough for a consistent production of the replicated structures. While the substrate passes through the exposing slit, a PDMS layer on the quartz cylinder and a cushion layer underneath the substrate can guarantee conformal contact between the mold and the substrate. As the UV light (365 nm wavelength and 1000 mW/cm<sup>2</sup> intensity) illuminates the passing substrate through the slit, complementary structures of the patterned PUA mold are generated continuously in the prepolymer layer, which are finished after the demolding process. As a result, a large area of flexible dry adhesive film (width of ~10 cm and thickness of ~100 μm) can be continuously fabricated, as demonstrated in Figure 1c.

To construct mushroom-shaped dry adhesives, PDMS or PU is widely used as they have advantageous mechanical properties

such as low elastic modulus and high elongation at break, which allows for simple and reliable prototyping (i.e., the easy demolding of the cured mushroomlike structures from a master without incurring any structural fracture).<sup>7,12,17,34,35</sup> Furthermore, the low elastic modulus of the PDMS and PU allows the replicated structures to make conformal contact with varying substrates even with a low preload and therefore exhibit a high level of adhesion strength in spite of the low surface energy of the PDMS and PU (see Tables 1 and 2). In spite of these advantages, PDMS and PU require long curing times at an increased temperature, as described above.<sup>7,12,17,34,35</sup>

To address this limitation and fabricate dry adhesive films by applying the continuous roll-to-roll process, we developed a modulated e-PUA with controlled mechanical and surface properties (see Tables 1 and 2). Compared with the PDMS or PU, the UV-curable e-PUA has several advantages, such as rapid prototyping with short curing time (<30 s), low energy consumption, and room temperature operation, therefore enabling rapid and scalable production of the dry adhesive films with uniform mushroomlike microstructures.<sup>18,20,39</sup> Furthermore, UV-curable materials typically show excellent resistance toward organic solvents, chemicals, heat, and tunable properties of the polymers, allowing for diverse applications.<sup>40</sup>



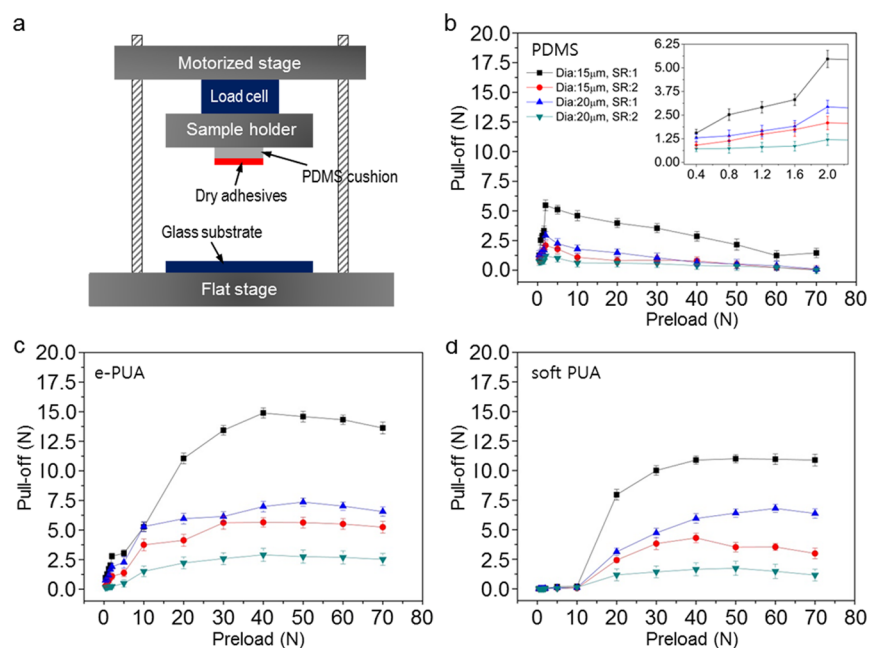
**Figure 3.** (a) Photograph showing the fabricated dry adhesive film having four different mushroomlike micropillars: (i) 17  $\mu\text{m}$  tip diameter, 15  $\mu\text{m}$  post diameter, and 30  $\mu\text{m}$  space, (ii) 22  $\mu\text{m}$  tip diameter, 20  $\mu\text{m}$  post diameter, and 40  $\mu\text{m}$  space, (iii) 17  $\mu\text{m}$  tip diameter, 15  $\mu\text{m}$  post diameter, and 15  $\mu\text{m}$  space, and (iv) 22  $\mu\text{m}$  tip diameter, 20  $\mu\text{m}$  post diameter, and 20  $\mu\text{m}$  space. (b) Optical microscopy and scanning electron microscopy (SEM) images corresponding to each micropillar.

Figure 2 presents the chemical formula of each ingredient, which includes the prepolymer (aliphatic urethane diacrylate oligomer), the modulators (bisphenol A (ethoxylated)-10-dimethacrylate (BPA(EO)10DMA) and tri(propylene glycol) diacrylate)), and the photoinitiator (2-hydroxy-2-methyl-1-phenylpropan-1-one). As shown in Tables 1 and 2, the e-PUA has a lower modulus than the soft PUA, whereas it exhibits high elongation at break similar to PDMS and also high surface energy, which are extremely advantageous properties in the development of bioinspired dry adhesives.<sup>40,41</sup> In particular, the use of the prepolymer having a heavy molecular weight (long chain length) makes it possible to provide a low cross-linking density, resulting in the good elongation characteristics of the cured polymer.<sup>40</sup> Furthermore, a linear long EO (ethoxylated) linkage in the BPA(EO)10DMA renders satisfactory flexibility, while most of the ethoxy group also provide high surface tension (42.6 dyn/cm), leading to a high level of adhesion. Tri(propylene glycol) diacrylate is a highly reactive and hydrophilic monomer with a low viscosity (15–20 cps). Therefore, combining the tri(propylene glycol) diacrylate with the oligomer results in a reduction of the mixture viscosity and therefore allows the mixture to fill the very fine structures in the micro- or nanoscale regime.

The mechanical properties of the e-PUA were determined by a universal testing machine (UTM, LR10K, Lloyd Instruments, England) with the mold prepared in the form of nonpatterned sheets for testing the tensile modulus and elongation at break. As shown in Table 1, the elongation at break of the e-PUA is about  $\sim 132.2\%$ , which is comparable to that of PDMS ( $\sim 146.0\%$ ). Furthermore, the elastic modulus of the e-PUA is about  $\sim 10.0$  MPa, which lies between that of soft PUA ( $\sim 19.8$  MPa) and PDMS ( $\sim 1.6$  MPa).<sup>40</sup> This means that the mushroomlike micropillars made of e-PUA have sufficient mechanical strength for structural integrity and repeatable use, yet they are also soft and flexible such that they can make close contact with the substrate over a large area, maximizing adhesion strength. In addition, the high elongation at break together with the low elastic modulus of the e-PUA prevent a structural failure in the demolding step (e.g., the tips of the pillars were torn from the master during demolding). In a recent report, we presented fast and successful replica molding of nanoscale structures to fabricate a dry adhesive, utilizing either commercially available hard (MINS-311RM, Minuta Tech) or soft PUA (MINS-301RM, Minuta Tech).<sup>18–20</sup>

However, it should be noted that we were not successful in fabrication of the mushroom-shaped microstructures using the hard or soft PUA. When we utilized the hard PUA, the cured PUA pillars stuck to the master and could not be removed. This was because the cured mushroom-shaped micropillars made of hard PUA were too stiff to be removed from the master possessing negative micropatterns. Especially, the protruding tips of the mushroom-shaped micropillars significantly hindered the success of the demolding step. When soft PUA was used, the cured PUA micropillars could be removed from the master because of the low elastic modulus ( $\sim 19.8$  MPa). However, most of the tips of the mushroom-shaped micropillars were torn off after the demolding step (see Supporting Information, Figure S1) mainly because of its low elongation at break ( $\sim 45.0\%$ ) (see Table 1). The main difference in the formulations of e-PUA, soft PUA, and hard PUA is the cross-linking modulator. The cross-linking modulator allows one to change the chain length or cross-linking density, which further leads to a modification in the mechanical properties. For hard PUA, trimethylolpropane (ethoxylated)-3-triacrylate (TMP-(EO)3TA) was chosen as the modulator since its relatively short chain length would lead to dense cross-linking.<sup>40</sup> For soft PUA, trimethylolpropane (ethoxylated)-15-triacrylate (TMP-(EO)15TA) was chosen because of its high number of ether linkages.<sup>40</sup> The long ether linkage can have a high degree of rotational movement that allows stretching. For e-PUA, bisphenol A (ethoxylated)-10-dimethacrylate (BPA(EO)-10DMA) was utilized, as shown in Figure 2. Owing to the difference in the number of reactive acrylates to be cross-linked, BPA(EO)10DMA leads to the formation of branched polymeric structures after photopolymerization, whereas (TMP(EO)15TA) induces the formation of network structures. BPA(EO)10DMA also has long chain lengths. As a result, e-PUA can exhibit a lower elastic modulus and a higher elongation at break than soft PUA.

Consequently, when we employed the e-PUA, large area dry adhesives in the form of a flexible film (width of  $\sim 10$  cm and thickness of  $\sim 500$   $\mu\text{m}$ ) could be generated in a continuous, scalable, and reliable manner by applying the roll-to-roll process, as demonstrated in Figures 1c and 3a. The production width was  $\sim 10$  cm, and the speed was about  $\sim 4$  cm/s; therefore, production capacity reached  $\sim 40$   $\text{cm}^2$   $\text{s}^{-1}$ . Note that this is the first demonstration of continuous production of the mushroom-shaped structures with UV-curable materials. Figure



**Figure 4.** (a) A schematic of adhesion measurement setup. (b–d) Measurement of pull-off force of fabricated mushroomlike micropillars made of (b) PDMS, (c) e-PUA, and (d) soft PUA for different preloads. The inset in (b) is a magnified view of pull-off forces with preloads ranging between 0 and 2 N. Here, the spacing ratio (SR) is defined as the distance between neighboring pillars divided by the post diameter.

3a presents the resulting dry adhesive film in which four different kinds of mushroomlike microstructures are embedded: micropillars with (i) 17  $\mu\text{m}$  tip diameter, 15  $\mu\text{m}$  post diameter, and 30  $\mu\text{m}$  space (spacing between neighboring pillars), (ii) 22  $\mu\text{m}$  tip diameter, 20  $\mu\text{m}$  post diameter, and 40  $\mu\text{m}$  space, (iii) 17  $\mu\text{m}$  tip diameter, 15  $\mu\text{m}$  post diameter, and 15  $\mu\text{m}$  space, and (iv) 22  $\mu\text{m}$  tip diameter, 20  $\mu\text{m}$  post diameter, and 20  $\mu\text{m}$  space. The height of the micropillars was about 20  $\mu\text{m}$ , and each micropillar had a patterned area of  $3 \times 3 \text{ cm}^2$ . Figure 3b shows optical microscopy and scanning electron microscopy (SEM) images corresponding to each replicated microstructure. As shown, mushroom-shaped micropillars with different pillar diameters and densities were successfully fabricated with good structural integrity and uniformity. Specifically, the spatulate flat head of the microstructures, which plays a significant role in enhancing adhesion strength, was successfully produced without any damage in spite of the continuous roll-type process. With our current roll-to-roll system, mushroom-shaped micropillars with heights of up to  $\sim 40 \mu\text{m}$  could be successfully generated. Higher micropillars could not be uniformly obtained because of structural fracture after the demolding process. A higher production speed ( $> \sim 4 \text{ cm/s}$ ) also could result in possible fracture of the spatulate tips during the demolding step. Further studies would be necessary to examine the influence of the structural height and rolling speed on the structural integrity of the fabricated dry adhesives.

Using the fabricated e-PUA micropillars, adhesion forces were measured against a smooth glass surface under a controlled preload of 0 to 70 N using custom-built equipment (Figure 4a). Also, the adhesion forces of micropillars made of PDMS and soft PUA were measured for comparison. Micropillar arrays made from hard PUA were excluded from the evaluation because of their low success rate of prototyping. For statistical significance, the adhesion measurement was carried out 20 times for each sample under identical conditions (i.e., relative humidity of 40% and ambient temperature of 25

$^{\circ}\text{C}$ ), and the averaged data were used. As shown in Figure 4b, the pull-off forces of PDMS micropillars were increased with an increase of the preload and maximized under a preload of 2 N. The maximum adhesion force was as high as  $\sim 5.5 \text{ N}$  ( $\sim 14.2 \text{ N cm}^{-2}$ ) for a micropillar array with 15  $\mu\text{m}$  post diameter and 15  $\mu\text{m}$  space. The maximum force was reduced to  $\sim 1.2 \text{ N}$  ( $\sim 3.1 \text{ N cm}^{-2}$ ) by increasing the pillar diameter to 20  $\mu\text{m}$  and space to 40  $\mu\text{m}$ . The pull-off of e-PUA micropillars also saturated as preload was increased and showed maximum values with preloads ranging between 40 and 50 N depending on the types of pillar arrays (Figure 4c). For example, the arrays with 15  $\mu\text{m}$  diameter and 15  $\mu\text{m}$  space exhibited maximum pull-off of  $\sim 14.9 \text{ N}$  ( $\sim 38.7 \text{ N cm}^{-2}$ ) with a preload of 40 N. The pull-off was slightly reduced with an increase of the preload to over 50 N. The increase of adhesion with a preload increase from 0.4 N to 40–50 N is attributed to the increase in actual contact area. The relatively high elastic modulus of the e-PUA ( $\sim 10 \text{ MPa}$ ) requires a higher preload to produce close contact between the e-PUA micropillars and the substrate and produce maximum adhesion strength. Furthermore, the PET supporting layer of the e-PUA adhesive has a high elastic modulus (2–3 GPa), which also increases the required preload to maximize the pull-off strength. On the other hand, the PDMS micropillars can make conformal contact even with a low preload because of the low tensile modulus of PDMS ( $\sim 1.6 \text{ MPa}$ ). The decrease of pull-off strength after passing the maximum point may be caused by the displacement of the micropillars due to the lateral deformation of the back film by the Poisson effect under an excessive preload.<sup>37</sup> The soft PUA micropillars showed similar adhesion tendency as that of e-PUA micropillars (Figure 4d). However, the soft PUA micropillars showed very low adhesion forces when the preload was lower than  $\sim 10 \text{ N}$ . Also, the overall adhesion forces were lower than the e-PUA arrays. This is because the soft PUA has a higher modulus than the e-PUA and the PDMS (Table 1), whereas it exhibits lower elongation at break than those two materials. This means that the dry

adhesives made of soft PUA are relatively stiffer than the e-PUA and the PDMS adhesives. As a result, the soft PUA adhesives require a high preload ( $>10$  N) to make conformal contact with a substrate and exhibit a pull-off force. More importantly, as described above, the tip structures of the soft PUA micropillars were mostly fractured during the demolding process, requiring repeated attempts to obtain successful samples. This signifies that the mechanical properties of the commercial soft PUA are not suitable for fabrication of dry adhesives with mushroomlike microstructures. Note that our additional adhesion tests showed that the pull-off forces of micropillars with mushroom-shaped tips were 2–4 times higher than those of micropillars with flat heads (Supporting Information, Figure S2).

In theory, the pull-off force for the flat tip ( $P_{\text{flat}}$ ) is given by<sup>11</sup>

$$P_{\text{flat}}(P_p) = N(P_p) \sqrt{8\pi K a^3 w_{12}} \quad (1)$$

where  $N(P_p)$  is the number of pillars in contact at preload  $P_p$ ,  $K$  is the effective Young's modulus of the system, and  $a$  is the radius of the flat tip. Here,  $w_{12}$  is the work of adhesion of the interface, which can be calculated with a harmonic mean equation as given by<sup>10,42</sup>

$$w_{12} = 4 \left( \frac{\gamma_1^d \gamma_2^d}{\gamma_1^d + \gamma_2^d} + \frac{\gamma_1^p \gamma_2^p}{\gamma_1^p + \gamma_2^p} \right) \quad (2)$$

where the superscripts d and p indicate the dispersion and polar components of the surface tension  $\gamma$ , respectively. With probe liquids of water and diiodomethane, the surface tension values can be obtained as summarized in Table 2.<sup>42</sup> From eqs 1 and 2, it can be seen that the pull-off force can be enhanced by using a material with low elastic modulus and high surface tension as it can maximize the number of micropillars in contact,  $N(P_p)$ , with a low preload and the work of adhesion ( $w_f$ ) at the microstructure/substrate interface. Accordingly, the mushroomlike micropillars fabricated from the e-PUA having lower elastic modulus and high surface tension can exhibit a high level of pull-off strength as compared to those made of soft PUA or PDMS. The high elongation of the e-PUA also contributes to the enhanced adhesion strength because of the increased surface conformation and extension during detachment.<sup>43</sup>

To explore practical applications of e-PUA micropillars produced by the roll-to-roll process, durability tests were carried out by repeating the cycles of attachment and detachment. A thin e-PUA dry adhesive (circular pad with 7 mm diameter) with spatulate micropillars (20  $\mu\text{m}$  diameter and 20  $\mu\text{m}$  space) was used for the test against a flat glass substrate with a preload of  $\sim 2$  N. Figure 5 shows the results of the durability test, which demonstrates that the pull-off force is maintained at  $\sim 1.9$  N without any notable reduction in adhesion capability even after more than 1000 cycles of attachment and detachment. With such remarkable retention of repeatable and reversible adhesion properties, the e-PUA adhesive pad has strong potential for use in semiconductor manufacturing processes, in which a very thin and fragile silicon (Si) wafer (thickness  $\approx 500$   $\mu\text{m}$ ) needs to be handled with high accuracy and precision without undergoing any surface contamination or damage.<sup>8,18,30</sup> To demonstrate the applicability of the e-PUA adhesives in semiconductor manufacturing, we developed an automated wafer transportation systems based on the adhesive pads. As shown in Figure 6a, five circular adhesive pads (7 mm diameter) with micropillar arrays having

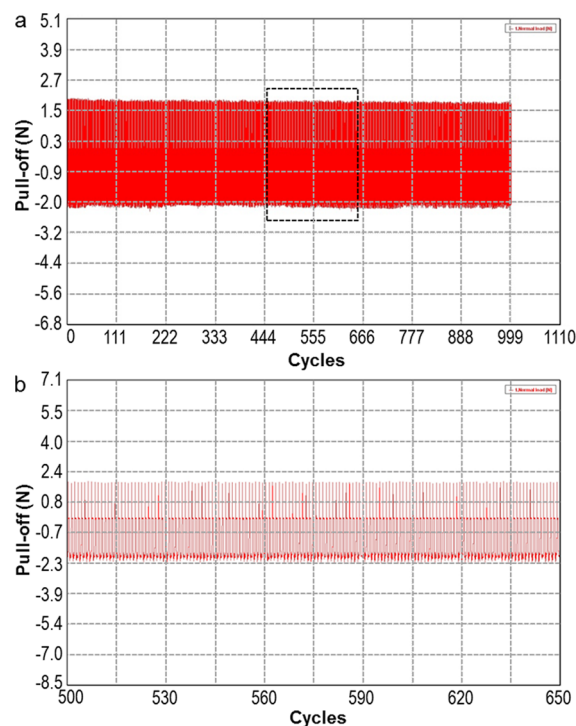


**Figure 5.** (a) Durability test of the e-PUA micropillars (20  $\mu\text{m}$  post diameter and 20  $\mu\text{m}$  space) over 1000 cycles of attachment and detachment. (b) Enlarged view of (a). A circular dry adhesive pad (7 mm diameter) was attached to a glass surface with a preload of  $\sim 2$  N.

20  $\mu\text{m}$  diameter and 20  $\mu\text{m}$  space (Figure 6b) were attached to a robotic arm that could move in three independent directions ( $z$ ,  $R$ , and  $\Theta$ ). Such a micropillar array was selected to achieve proper adhesion strength ( $\sim 0.7$  N per single pad) that can prevent a substrate from sliding during fast transportation and enable easy detachment of the substrate during the separation stage under a preload ( $\sim 1.25$  N), which is the weight of a Si wafer 300 mm in diameter ( $\sim 128$  g). One of the biggest advantages of such a structured adhesive is that the pull-off force can be precisely controlled by modulating the geometries of the pillar arrays (e.g., diameter and density). Note that when we used a nonstructured PDMS slab or a patterned adhesive pad with a higher pull-off force, the wafer wobbled significantly during the separation stage, which could eventually induce damage to the Si wafer. Figure 6c shows time-lapse images depicting the automated transportation of a Si wafer utilizing the e-PUA adhesives. As shown, the robotic arm equipped with the pads can make a firm attachment with the wafer by simply approaching the backside of the wafer even under a low preload ( $\sim 1.25$  N). After forming a firm attachment, the automated system could transport the substrate without causing any substrate sliding. In general, the level of substrate sliding is required to be within 0.3 mm for semiconductor manufacturing. To this end, we performed sliding tests utilizing the e-PUA dry adhesives. The position of the wafer was examined after transportation with a laser sensor that checks the peripheral alignment of the wafers loaded in a target location. Test results indicated that the substrate sliding was maintained within 0.06 mm over 10 000 cycles of attachment and detachment (Supporting Information, Figure S3). After arriving at a target cassette, the wafer was smoothly separated from the adhesive pads by moving the arm downward with the aid of a cassette guide (see the Video in the Supporting Information). The

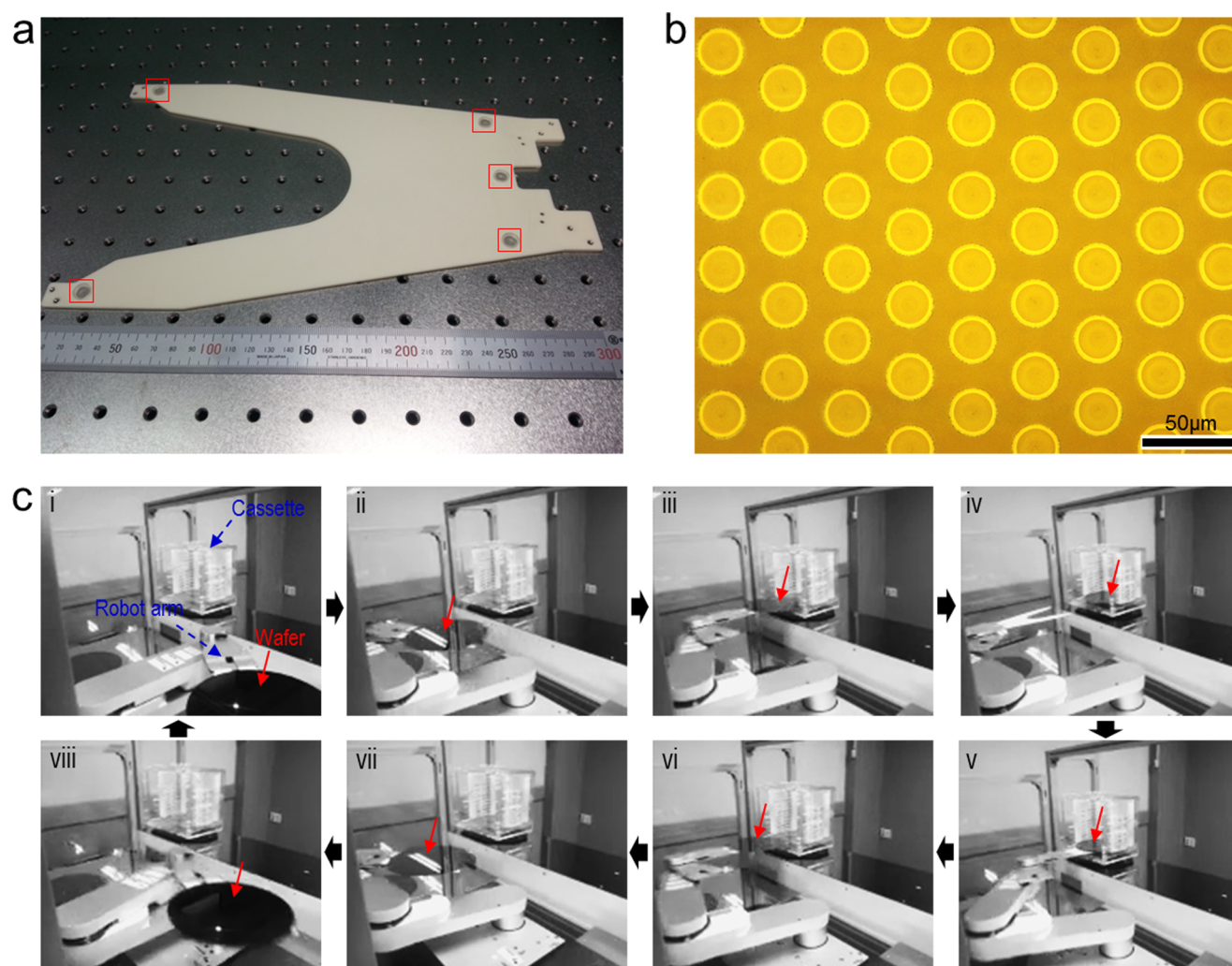


**Figure 6.** (a) Wafer holder equipped with five circular dry adhesive pads. (b) Optical microscopy image of the pads. (c) Time-lapse images showing the automated transportation of a 300 mm Si wafer. The wafer was successfully transported and handled without any sliding or damage problems over 10 000 cycles of attachment and detachment.

wafer was successfully handled without any significant problems (e.g., substrate sliding, contamination, or damage) over 10 000 cycles of attachment and detachment, demonstrating the strong potential of the dry adhesive pads for use in precision manufacturing industries.

## CONCLUSIONS

In summary, we have presented a simple yet scalable strategy for fabricating dry adhesives with mushroom-shaped micropillars by a combination of the roll-to-roll process and the use of a modulated UV-curable resin. The modulated resin has a low tensile modulus ( $\sim 10.0$  MPa) and a high elongation-at-break ( $\sim 132.2\%$ ), comparable to PDMS, and it can be cured at room temperature in a few seconds similar to commercial PUA resins. As a result, a large-area dry adhesive in the form of a thin flexible sheet can be produced in a highly continuous and scalable manner without structural defects. The fabricated dry adhesives with mushroom-shaped microstructures exhibit a strong pull-off strength of up to  $\sim 38.7$  N  $\text{cm}^{-2}$  on the glass surface as well as high durability without any noticeable degradation. Furthermore, an automated substrate transportation system equipped with the dry adhesives can transport a 300 mm Si wafer over 10 000 repeating cycles with high

accuracy. This new approach can thus prove valuable for the industrialization and commercialization of bioinspired smart dry adhesives in a variety of applications including precision and clean manufacturing.

## ASSOCIATED CONTENT

### Supporting Information

Optical microscopy images of the fractured mushroom-shaped micropillars made of soft PUA. Measurement of pull-off force of fabricated micropillars with flat heads made of PDMS, e-PUA, and soft PUA for different preloads. Wafer sliding tests utilizing the e-PUA dry adhesives. Video clip showing the automated transportation of a 300 mm Si wafer. This material is available free of charge via the Internet at <http://pubs.acs.org>.

## AUTHOR INFORMATION

### Corresponding Authors

\*E-mail: hoonejeong@unist.ac.kr. (H.E.J.)

\*E-mail: mkkwak@knu.ac.kr. (M.K.K.)

### Author Contributions

<sup>†</sup>H. Yi and I. Hwang contributed equally to this work.

### Notes

The authors declare no competing financial interest.



## ACKNOWLEDGMENTS

This work was supported by the Ulsan National Institute of Science and Technology (UNIST) through the Creativity and Innovation Project Program (Grant No. UMI 1.140012.01), the MOTIE/KEIT Program (Grant No. 10045070), and the Young Researchers Supporting Program through the National Research Foundation of Korea (NRF) funded by the Ministry of Education, Science and Technology (2013R1A1A1061219 and 2012R1A1A1040040).

## DEDICATION

This work is dedicated to the late Prof. K.-Y. Suh who was a mentor to us.

## REFERENCES

- (1) Gorb, S. N.; Varenberg, M. Mushroom-Shaped Geometry of Contact Elements in Biological Adhesive Systems. *J. Adhes. Sci. Technol.* **2007**, *21*, 1175–1183.
- (2) Autumn, K.; Liang, Y. A.; Hsieh, S. T.; Zesch, W.; Chan, W. P.; Kenny, T. W.; Fearing, R.; Full, R. J. Adhesive Force of a Single Gecko Foot-Hair. *Nature* **2000**, *405*, 681–685.
- (3) Autumn, K.; Sitti, M.; Liang, Y. C. A.; Peattie, A. M.; Hansen, W. R.; Sponberg, S.; Kenny, T. W.; Fearing, R.; Israelachvili, J. N.; Full, R. J. Evidence for Van Der Waals Adhesion in Gecko Setae. *Proc. Natl. Acad. Sci. U. S. A.* **2002**, *99*, 12252–12256.
- (4) Federle, W. Why Are So Many Adhesive Pads Hairy? *J. Exp. Biol.* **2006**, *209*, 2611–2621.
- (5) Arzt, E.; Gorb, S.; Spolenak, R. From Micro to Nano Contacts in Biological Attachment Devices. *Proc. Natl. Acad. Sci. U. S. A.* **2003**, *100*, 10603–10606.
- (6) Gorb, S.; Varenberg, M.; Peressadko, A.; Tuma, J. Biomimetic Mushroom-Shaped Fibrillar Adhesive Microstructure. *J. R. Soc., Interface* **2007**, *4*, 271–275.
- (7) del Campo, A.; Greiner, C.; Alvarez, I.; Arzt, E. Patterned Surfaces with Pillars with Controlled 3d Tip Geometry Mimicking Bioattachment Devices. *Adv. Mater.* **2007**, *19*, 1973–1977.
- (8) Jeong, H. E.; Suh, K. Y. Nanohairs and Nanotubes: Efficient Structural Elements for Gecko-Inspired Artificial Dry Adhesives. *Nano Today* **2009**, *4*, 335–346.
- (9) Majidi, C.; Groff, R. E.; Maeno, Y.; Schubert, B.; Baek, S.; Bush, B.; Maboudian, R.; Gravish, N.; Wilkinson, M.; Autumn, K.; Fearing, R. S. High Friction from a Stiff Polymer Using Microfiber Arrays. *Phys. Rev. Lett.* **2006**, *97*.
- (10) Jeong, H. E.; Lee, S. H.; Kim, P.; Suh, K. Y. Stretched Polymer Nanohairs by Nanodrawing. *Nano Lett.* **2006**, *6*, 1508–1513.
- (11) Greiner, C.; del Campo, A.; Arzt, E. Adhesion of Bioinspired Micropatterned Surfaces: Effects of Pillar Radius, Aspect Ratio, and Preload. *Langmuir* **2007**, *23*, 3495–3502.
- (12) Kim, S.; Sitti, M. Biologically Inspired Polymer Microfibers with Spatulate Tips as Repeatable Fibrillar Adhesives. *Appl. Phys. Lett.* **2006**, *89*, 261911.
- (13) Autumn, K.; Dittmore, A.; Santos, D.; Spenko, M.; Cutkosky, M. Frictional Adhesion: A New Angle on Gecko Attachment. *J. Exp. Biol.* **2006**, *209*, 3569–3579.
- (14) Kwak, M. K.; Jeong, H. E.; Kim, T. I.; Yoon, H.; Suh, K. Y. Bio-Inspired Slanted Polymer Nanohairs for Anisotropic Wetting and Directional Dry Adhesion. *Soft Matter* **2010**, *6*, 1849–1857.
- (15) Santos, D.; Spenko, M.; Parness, A.; Kim, S.; Cutkosky, M. Directional Adhesion for Climbing: Theoretical and Practical Considerations. *J. Adhes. Sci. Technol.* **2007**, *21*, 1317–1341.
- (16) Lee, J. H.; Fearing, R. S.; Komvopoulos, K. Directional Adhesion of Gecko-Inspired Angled Microfiber Arrays. *Appl. Phys. Lett.* **2008**, *93*.
- (17) Murphy, M. P.; Aksak, B.; Sitti, M. Gecko-Inspired Directional and Controllable Adhesion. *Small* **2009**, *5*, 170–175.
- (18) Jeong, H. E.; Lee, J. K.; Kim, H. N.; Moon, S. H.; Suh, K. Y. A Nontransferring Dry Adhesive with Hierarchical Polymer Nanohairs. *Proc. Natl. Acad. Sci. U. S. A.* **2009**, *106*, 5639–5644.
- (19) Jeong, H. E.; Lee, J. K.; Kwak, M. K.; Moon, S. H.; Suh, K. Y. Effect of Leaning Angle of Gecko-Inspired Slanted Polymer Nanohairs on Dry Adhesion. *Appl. Phys. Lett.* **2010**, *96*.
- (20) Kim, T. I.; Jeong, H. E.; Suh, K. Y.; Lee, H. H. Stopped Nanohairs: Geometry-Controllable, Unidirectional, Reversible, and Robust Gecko-Like Dry Adhesive. *Adv. Mater.* **2009**, *21*, 2276–2281.
- (21) Aksak, B.; Murphy, M. P.; Sitti, M. Adhesion of Biologically Inspired Vertical and Angled Polymer Microfiber Arrays. *Langmuir* **2007**, *23*, 3322–3332.
- (22) Reddy, S.; Arzt, E.; del Campo, A. Bioinspired Surfaces with Switchable Adhesion. *Adv. Mater.* **2007**, *19*, 3833–3837.
- (23) Northen, M. T.; Greiner, C.; Arzt, E.; Turner, K. L. A Gecko-Inspired Reversible Adhesive. *Adv. Mater.* **2008**, *20*, 3905–3909.
- (24) Greiner, C.; Arzt, E.; del Campo, A. Hierarchical Gecko-Like Adhesives. *Adv. Mater.* **2009**, *21*, 479–482.
- (25) Lin, P. C.; Vajpayee, S.; Jagota, A.; Hui, C. Y.; Yang, S. Mechanically Tunable Dry Adhesive from Wrinkled Elastomers. *Soft Matter* **2008**, *4*, 1830–1835.
- (26) Parness, A.; Soto, D.; Esparza, N.; Gravish, N.; Wilkinson, M.; Autumn, K.; Cutkosky, M. A Microfabricated Wedge-Shaped Adhesive Array Displaying Gecko-Like Dynamic Adhesion, Directionality and Long Lifetime. *J. R. Soc., Interface* **2009**, *6*, 1223–1232.
- (27) Yoon, H.; Jeong, H. E.; Kim, T. I.; Kang, T. J.; Tahk, D.; Char, K.; Suh, K. Y. Adhesion Hysteresis of Janus Nanopillars Fabricated by Nanomolding and Oblique Metal Deposition. *Nano Today* **2009**, *4*, 385–392.
- (28) Kwak, M. K.; Pang, C.; Jeong, H. E.; Kim, H. N.; Yoon, H.; Jung, H. S.; Suh, K. Y. Towards the Next Level of Bioinspired Dry Adhesives: New Designs and Applications. *Adv. Funct. Mater.* **2011**, *21*, 3606–3616.
- (29) Stork, N. E. The Adherence of Beetle Tarsal Setae to Glass. *J. Nat. Hist.* **1983**, *17*, 583–597.
- (30) Zhou, M.; Tian, Y.; Sameoto, D.; Zhang, X. J.; Meng, Y. G.; Wen, S. Z. Controllable Interfacial Adhesion Applied to Transfer Light and Fragile Objects by Using Gecko Inspired Mushroom-Shaped Pillar Surface. *ACS Appl. Mater. Interfaces* **2013**, *5*, 10137–10144.
- (31) Wang, Y.; Hu, H.; Shao, J. Y.; Ding, Y. C. Fabrication of Well-Defined Mushroom-Shaped Structures for Biomimetic Dry Adhesive by Conventional Photolithography and Molding. *ACS Appl. Mater. Interfaces* **2014**, *6*, 2213–2218.
- (32) Heepe, L.; Kovalev, A. E.; Filippov, A. E.; Gorb, S. N. Adhesion Failure at 180 000 Frames Per Second: Direct Observation of the Detachment Process of a Mushroom-Shaped Adhesive. *Phys. Rev. Lett.* **2013**, *111*.
- (33) Jeong, H. E.; Kwak, M. K.; Suh, K. Y. Stretchable, Adhesion-Tunable Dry Adhesive by Surface Wrinkling. *Langmuir* **2010**, *26*, 2223–2226.
- (34) Kwak, M. K.; Jeong, H. E.; Bae, W. G.; Jung, H. S.; Suh, K. Y. Anisotropic Adhesion Properties of Triangular-Tip-Shaped Micropillars. *Small* **2011**, *7*, 2296–2300.
- (35) Sameoto, D.; Menon, C. Direct Molding of Dry Adhesives with Anisotropic Peel Strength Using an Offset Lift-Off Photoresist Mold. *J. Microchem. Microeng.* **2009**, *19*.
- (36) Seo, S.; Lee, J.; Kim, K. S.; Ko, K. H.; Lee, J. H.; Lee, J. Anisotropic Adhesion of Micropillars with Spatula Pads. *ACS Appl. Mater. Interfaces* **2014**, *6*, 1345–1350.
- (37) Bae, W. G.; Kim, D.; Suh, K. Y. Instantly Switchable Adhesion of Bridged Fibrillar Adhesive Via Gecko-Inspired Detachment Mechanism and Its Application to a Transportation System. *Nanoscale* **2013**, *5*, 11876–11884.
- (38) Ok, J. G.; Kwak, M. K.; Huard, C. M.; Youn, H. S.; Guo, L. J. Photo-Roll Lithography (PRL) for Continuous and Scalable Patterning with Application in Flexible Electronics. *Adv. Mater.* **2013**, *25*, 6554–6561.
- (39) Choi, S. J.; Yoo, P. J.; Baek, S. J.; Kim, T. W.; Lee, H. H. An Ultraviolet-Curable Mold for Sub-100-Nm Lithography. *J. Am. Chem. Soc.* **2004**, *126*, 7744–7745.

(40) Choi, S. J.; Kim, H. N.; Bae, W. G.; Suh, K. Y. Modulus- and Surface Energy-Tunable Ultraviolet-Curable Polyurethane Acrylate: Properties and Applications. *J. Mater. Chem.* **2011**, *21*, 14325–14335.

(41) Bhatia, Q. S.; Chen, J. K.; Koberstein, J. T.; Sohn, J. E.; Emerson, J. A. The Measurement of Polymer Surface-Tension by Drop Image-Processing - Application to PDMS and Comparison with Theory. *J. Colloid Interface Sci.* **1985**, *106*, 353–359.

(42) Wu, S. *Polymer Interface and Adhesion*; Marcel Dekker: New York, NY, 1982.

(43) Murphy, M. P.; Kim, S.; Sitti, M. Enhanced Adhesion by Gecko-Inspired Hierarchical Fibrillar Adhesives. *ACS Appl. Mater. Interfaces* **2009**, *1*, 849–855.